FINAL REPORT

19 November 2021

Ecological value of lands in the Shasta-Trinity National Forest

Submitted to: The Pew Charitable Trusts

1. INTRODUCTION

Identifying areas of high ecological value is critical to prioritizing new conservation efforts, but remains a considerable challenge given multiple land use objectives, the variety of ecological and environmental benefits that any given landscape might provide (e.g., carbon storage, wildlife habitat, ecological connectivity), and potential trade-offs between these benefits. In an effort to support the US Forest Service's (USFS) ongoing revisions of its Land and Resource Management Plans (commonly called 'forest plans'), we have calculated the relative ecological value of lands in Shasta-Trinity National Forest based on a collection of key spatial data sets. We define 'ecological value' as the potential for a given location on the landscape (i.e., a pixel in a gridded landscape raster) to contribute to crucial ecological processes such as supporting biodiversity and connectivity and buffering organisms against the impacts of climate change through carbon storage and accessibility of favorable climate conditions. This concept is related to that of 'conservation value,' as used by Dickson et al. (2014), but does not directly incorporate social/political aspects of conservation such as the proportion of an ecosystem type currently protected.

Here we describe our work integrating multiple key ecological and environmental variables (hereafter, "indicators") into a composite index that provides a single coherent measure of ecological value for each location across the national forest (excluding national grasslands at the Ranger District level where appropriate). We applied an innovative approach to address correlations between ecological indicators and ensure that index values are as interpretable as possible. Our analysis considers all lands within the administrative boundary of the national forest, regardless of ownership (e.g., federal, state, private). Because many of the ecological processes that our indicator variables estimate (e.g., ecological connectivity and the ability for species to move in response to climate change) are influenced by the surrounding landscape, non-NFS lands interspersed within national forest boundaries will affect the overall ecological value of lands within the forest. For instance, modified private lands within a national forest boundary may impact the capacity of the broader landscape to support the movement of organisms. We therefore chose to include all ownership types within national forest boundaries when estimating the average value of indicator variables and the composite index. This report focuses on currently unprotected lands within the Shasta-Trinity National Forest and identifies areas in the top 10% of ecological value.

2. INDICATORS

The set of ecological and environmental indicators used in this analysis was selected based on previous work by Conservation Science Partners (Dickson et al. 2014) and was co-developed with staff at The Pew Charitable Trusts to best capture the range of ecological values represented within lands managed by the US Forest Service. We chose a contemporary, parsimonious set of indicators that represent key conservation priorities related to biodiversity and climate mitigation. We endeavored to

keep our indicator set sufficiently concise to ensure that it is clear to users what information is being integrated into each index and to maximize interpretability of resulting index values. We also ensured indicators were based on the best quality spatial data (i.e., maps or 'layers') available and derived at a relatively high spatial resolution. The selected indicators are described below.

Total carbon estimates the total ecosystem carbon (above and below ground biomass, soil organic carbon) that currently exists in a given location in units of metric tons of carbon per hectare. This 300-meter resolution dataset represents the best available information on current carbon storage (circa 2010) across the US (Spawn et al. 2020, Noon et al. in press). Total carbon was determined based on ecosystem type, using the average carbon content per hectare for each of 13 terrestrial biomes and three coastal biomes (Goldstein et al. 2020). Ecosystem-specific values of average above ground biomass carbon per hectare were derived from applicable databases (e.g., ForC database of forest carbon stocks [Anderson-Teixeira et al. 2018] and global grassland carbon database [Xia et al. 2014]), while below ground biomass carbon was estimated for each ecosystem type based on below ground to above ground (root:shoot) biomass ratios (Mokany et al. 2006) for the dominant vegetation type in that system. Soil organic carbon stocks were estimated using the SoilGrids database (Hengl et al. 2017). **Note:** Recent research indicates that changes in albedo (i.e., amount of solar radiation reflected by snow or light-colored bare ground) may reduce the effective carbon benefits of forest cover in parts of the western U.S., including the Rocky Mountains region - forest loss in this region will lead to climate warming due to carbon release, but this may be offset by increased cooling through greater solar reflectance in cleared areas (Mykleby et al. 2017, Williams et al. 2021).

Climate resilience estimates the degree to which the climate conditions currently experienced by a species will be accessible in the future. Areas of high climate resilience are those that contribute to the ability of species to adapt to climate change through both local and long-distance movements. Climate resilience is derived as the multiplicative inverse of climate velocity, a measure of the instantaneous velocity of climate change at a location on the landscape (Carroll et al. 2015). The climate velocity metric used here was originally developed by Hamann et al. (2015) and expanded by the AdaptWest Project (2015) by integrating 11 climate variables via principal component analysis (PCA) and calculating velocity based on the distance between sites with matching present climate (averaged from 1981 to 2010) and future climate (2055, based on RCP8.5 emissions scenario). The 1-km resolution climate variables in the PCA include (see Hamann et al. 2015 for further details on climate variables):

1. Mean annual temperature
2. Mean temperature of the warmest month (MTW)
3. Mean temperature of the coldest month (MTC)
4. Difference between MTC and MTW
5. Mean annual precipitation
6. Mean summer (May to September) precipitation
7. Mean winter (October to April) precipitation

8. Degree-days above 5°C
9. Number of frost-free days
10. Hargreave's reference evaporation
11. Hargreave's climatic moisture index

The Hamann et al. (2015) algorithm can be implemented in either forward (find future climate locations matching the focal location's current climate) or backward (find current climate locations matching the focal location's future climate) directions. We derived our estimate of climate resilience based on backward velocity, which asks: given the projected future climate habitat of a focal location, what is the minimum distance an organism has to migrate to colonize this climate habitat?

Imperiled species richness estimates the number of species of conservation concern likely to occur in a given area. This layer, developed by NatureServe, integrates habitat suitability maps for 2,216 of the nation's most imperiled species, including "vertebrates (birds, mammals, amphibians, reptiles, freshwater fishes; 309 species), freshwater invertebrates (228 species), pollinators (43 species), and vascular plants (1,636 species)" (NatureServe 2020). This 990-m resolution layer includes species designated by NatureServe as imperiled or critically imperiled, and species listed as threatened or endangered under the Endangered Species Act.

Vertebrate species richness estimates the number of terrestrial, non-volant species likely to occur in a given area. Following Soto-Navarro et al. (Soto-Navarro et al. 2020), we calculated species richness by overlaying IUCN range maps for amphibians, reptiles, and mammals and restricted these ranges based on recently published maps of IUCN habitat (Jung et al. 2020). Richness maps were produced at 2km resolution, as recommended for IUCN range data (KBA 2019).

Ecological intactness estimates the degree to which a given location remains in a natural state. Ecologically intact landscapes are those with minimal or no influence from human activities and which are therefore able to support natural evolutionary and ecological processes (Angermeier and Karr 1996, Parrish et al. 2003) as well as communities of organisms similar in species composition, diversity, and functional organization to those of undisturbed habitats (Parrish et al. 2003). Ecological intactness is calculated as *1 - L*, where *L* is the intensity of human land use (Theobald 2013). Drawing on our previous work (CSP 2019), we derived estimates of anthropogenic impact (circa 2017), quantifying the intensity *and* footprint of human land use based on multiple types of human activities, including residential and commercial development, agriculture, energy production and mining, transportation, and harvest of forest products (CSP 2019). Ecological intactness was derived for the conterminous US at 90-m resolution.

Ecological connectivity estimates the ability of a given location to support the natural movement of organisms through processes such as dispersal, migration, and gene flow and to provide linkages between areas of high-quality habitat (Dickson et al. 2017). Maintaining areas of high ecological connectivity is also considered a key strategy for supporting species migrations and range shifts under

climate change (Heller and Zavaleta 2009). We used the procedure described by Dickson et al. (2017) to derive resistance surfaces for connectivity models by rescaling our anthropogenic impact layer (described above under ecological intactness) and incorporating a realistic penalty for steep slopes, which may present barriers to movement for many organisms. We used a mammal species richness layer to estimate source strength (the likelihood that a given location will act as starting/end point for animal movement), treating source strength as proportional to the number of mammal species estimated to occur in a given location. As above, we estimated mammal richness by overlaying IUCN range maps for mammals (408 species) and restricting these ranges based on recently published maps of IUCN habitat (Jung et al. 2020). Richness maps were produced at 2-km resolution, as recommended for IUCN range data. We used a circuit theory-based approach (McRae et al. 2008, Dickson et al. 2019) to model the flow of organisms across conterminous US, using Omniscape software to implement an omni-directional connectivity model at 1-km resolution (McRae et al. 2016, Landau et al. 2021).

Vegetation diversity describes the diversity of plant communities, defined here as groups of "plant community types (associations) that tend to co-occur within landscapes with similar ecological process, substrates, and/or environmental gradients" (Comer et al. 2003). Such plant communities provide a variety of habitats essential for maintaining broader species diversity (Noss 1990). Vegetation diversity may stem from the presence of strong elevation gradients, ecotonal transitions among biome types, and/or interspersion of unique water-associated communities, such as wetlands, marshlands, meadows, and riparian zones. We used data on vegetation type from the 30-m resolution USGS Gap Ecological Systems data layer (USGS 2011) as the basis for calculating vegetation diversity and assigned null values to all developed and invasive species land cover types prior to running the analysis such that these lands would not contribute toward the diversity calculation. Following Theobald et al. (2015) we estimated vegetation diversity using the Shannon-Weaver equitability index (a normalized version of the Shannon-Weaver diversity index; Theobald et al. 2015) based on the proportion of pixels within a given neighborhood that were classified as a particular vegetation type. We estimated vegetation diversity across multiple spatial scales using moving window neighborhood sizes that ranged between a radius of 1.2 and 115.8 km, corresponding to the average area of USGS hydrologic units (Hydrologic Unit Codes 4-16; Theobald et al. 2015). The final diversity value was derived by taking the average across all spatial scales. Values have a theoretical range of zero to one with higher value denoting places of greater vegetation diversity.

3. THE COMPOSITE INDEX

The indicator variables described above were integrated into a composite index, providing a single estimate of ecological value for each location (i.e., pixel) within the national forest. As described in further detail below, we developed our composite index using indicator values from all lands within national forest boundaries across the conterminous US (CONUS) and then use this composite index of ecological value to identify unprotected areas of highest ecological value within the Shasta-Trinity National Forest. Note that some USFS administrative units also contain national grasslands, which may

have indicator values that differ substantially from those of national forests in the same unit. These national grasslands were excluded from our analysis at the Ranger District level.

Composite indices are mathematical combinations of (in this case) ecological and environmental variables that otherwise have no common meaningful unit of measurement (Burgass et al. 2017). There are several key decisions related to how indicator values are mathematically combined in a composite index – including whether and how indicators are transformed, aggregated, and weighted – that will affect the ultimate interpretation of index values and resulting planning and prioritization decisions (Burgass et al. 2017, Greco et al. 2019). Here we describe our efforts to develop a transparent and well-justified approach to deriving the composite index, paying special attention to the issue of indicator weights, a complicated problem given the often considerable difference between an indicator's weight and it's actual influence on the resulting index value (Becker et al. 2017).

The first major decision we addressed was whether and how to transform indicator variables. Some investigators choose to nominally "normalize" highly skewed variables by applying certain transformations. However, such transformations, by definition, change the values of an indicator and its behavior and influence in a composite index. Lacking strong justification for any particular transformation, we choose not to alter the distributions of any of the indicators.

The next decision concerned the mathematical function used to place all indicators on a common scale. This step is necessary because the indicators we used have non-comparable units (e.g., metric tons of carbon per hectare, number of vertebrate species). To ensure comparability across indicators, each indicator was standardized (converted to z-scores) by

$$z_{ij} = \frac{x_{ij} - mean(x_j)}{sd(x_j)},$$
(eq. 1)

where x_{ij} is the vector of $i = 1, 2, …, N$, observations of indicator j and z_{ij} are the z-transformed values. Converting to z-scores has the effect of centering the distribution of each indicator on zero and converting the unit of measurement for all indicators to standard deviations, allowing direct comparison between indicators with very different native units. We performed indicator standardization based on the mean and standard deviation of indicator values across all pixels within the boundaries of all administrative units in the conterminous US. Each standardized indicator had a mean of zero, corresponding to the average value of that indicator across the entire extent of this analysis, and ranged between approximately -4 and 4 (with the exact range differing somewhat between indicators).

Finally, we calculated the value of the composite index, *y*, at each location, *i*, across all national forests as the weighted linear combination of indicator variables. We used a weighted mean of indicators (Paruolo et al. 2013, Becker et al. 2017) such that

$$y_i = \sum_{j=1}^{J} z_{ij} w_j,$$ (eq. 2)

where w_j is the weight applied to indicator *j*, with weights summing to 1 across all indicators. It is tempting to assume that the weights represent the relative importance of each indicator in determining the overall composite index, but this is not always the case (Paruolo et al. 2013, Becker et al. 2017). When indicators are correlated, as environmental variables and metrics often are, weights are often not directly equivalent to, or even intuitively predictive of, indicator 'importance,' which we define as the degree to which a single indicator can explain observed variation in the composite index (see **Appendix A** for a mathematical definition of importance). Note that similar problems can also occur when indicators do not have equal variance, however, this is not relevant in our analysis because, as described above, all indicators were standardized by converting to z-scores. Given the complex relationship between weights and influence, the naive application of weights can lead to non-intuitive composite index values for which particular indicators are more or less influential than expected. Therefore, rather than simply basing our analysis on equal weighting of each indicator, as is frequently done in analyses aggregating multiple ecological datasets, we instead adapted a method proposed by Becker et al. (2017) to determine the set of weights needed to achieve *equal importance* across all indicator variables. This approach, which involves using an optimization algorithm to find the set of weights that yields a predetermined importance value for each indicator, is described in detail in **Appendix A**. Our optimized weights approach thus allows for readily interpretable composite index scores in which all indicator variables are essentially placed on equal footing in determining the value of the index at any given location. It is worth noting that other weighting schemes are also valid (e.g., some indicators could be made twice as important as others) and that our choice of weights providing equal importance is a subjective one. However, in the absence of *a priori* assumptions regarding differential importance between indicators, we have chosen to equalize importance across indicators. We calculated the composite index in Google Earth Engine (GEE) at 90-m resolution. Prior to analysis, all indicator variables were resampled to 90-m resolution using GEE's default nearest-neighbor algorithm.

4. IDENTIFYING AREAS OF HIGHEST ECOLOGICAL VALUE

As noted above, the composite index of ecological value was calculated across all national forests in the coterminous United States. To identify the highest relative value areas within the Shasta-Trinity National Forest, we first clipped the pixel-level composite index results to just this forest and used a circular kernel to calculate the focal mean within a 5,000-acre area around each pixel. This smoothing

process retained the original data resolution but ensured that any pixels identified as high ecological value (i.e., high values of the composite index) actually represent high value areas within the broader region. We chose an area of 5,000 acres to correspond with size requirements contained in multiple US public lands statutes and associated agency regulations and guidance (e.g., Forest Service Land Management Planning Handbook 1909.12, Wilderness Act of 1964). We identified existing protected areas within the National Forest (i.e., lands categorized as GAP 1 or 2 protection status in the USGS Protected Areas Database of the U.S., version 2.1) and excluded these from the smoothed composite index surface. We then identified all remaining pixels falling within the top 10% of smoothed composite index values across all unprotected areas of the national forest and drew polygons around contiguous groups of pixels within this top 10% category. The resulting polygons represent High Ecological Value Areas (HEVAs) that can serve as targets for additional conservation-focused management. HEVAs are similar to Conservation Priority Areas, as defined by Dixon et al. (2014), but focus specifically on ecological value rather than incorporating social/political aspects of conservation. Note that, while the HEVAs are based on the composite index layer that has been smoothed to 5,000 acres, the polygons themselves can be of any size, depending on the number of contiguous high value pixels in the smoothed index layer. To remove potential artifacts and polygons that are too small to be of relevance to management, we filtered the set of HEVA polygons to only those with an area greater than 100 acres. This 100-acre cut-off, while arbitrary, will help to focus our results on larger areas that may be better suited for conservation-oriented management.

For each HEVA, we calculated the average (± standard deviation) value of each indicator and the composite index across all pixels falling within the HEVA polygon. As noted above, this analysis (including the delineation of HEVAs) was performed using all lands within National Forest administrative boundaries, regardless of ownership type. We therefore also calculated the proportion of each HEVA comprised of National Forest System (NFS) lands (i.e., those owned by USFS). NFS lands were identified using the Surface Ownership Parcels dataset available at https://data.fs.usda.gov/geodata.

Finally, to aid in the comparison of relative ecological value between different HEVAs, we developed an estimate of relative road impacts within each HEVA. We started by compiling a comprehensive dataset of all roads and all trails on which motor vehicle use is allowed. We used the U.S. Census Bureau's TIGER roads dataset (U.S. Census Bureau, 2019), which represents all major roads and local routes, and the USFS Motor Vehicle Use Map (MVUM) roads and trails datasets (available at https://data.fs.usda.gov/geodata), which represent roads and trails managed by USFS. It is important to note that the ecological impacts of a road occur beyond the physical road itself, influencing factors such as vegetation structure and wildlife movement in a zone extending out from the road edge (Forman and Alexander 1998, Shanley and Pyare 2011). The actual size of this road effect zone varies substantially depending on the species or ecological process being considered and features of the road itself (e.g., traffic volume) but may in some cases be >100m (Forman 2000). For this analysis, we rasterized all

roads at 30-m resolution, thus considering the road effect zone to be 30-m wide, a conservative value that corresponds to the actual footprint of some larger roads (Theobald 2010, 2013) and is well within the size range of road effect zones estimated by previous studies (Forman 2000, Shanley and Pyare 2011). We then calculated an estimate of relative road impacts for each HEVA as the total area of all 30-m wide roads within a given HEVA divided by total HEVA area. Importantly, our road impacts metric is not an estimate of road density (i.e., length of road per unit area) but rather a relative estimate of the proportion of each HEVA that is impacted by the ecological effects of roads. This value is comparable across HEVAs. It is also worth noting that there is some overlap between the TIGER and MVUM roads datasets such that some routes are represented by line features in both datasets. Treating all roads as being 30-m wide, as done here, mitigates the effects of double counting routes represented in both datasets, which would occur if our estimates were instead based on road length.

5. RESULTS AND CONSIDERATIONS

Figure 1 shows the smoothed composite index mapped across the Shasta-Trinity National Forest, highlighting the locations of each HEVA. We identified 12 HEVAs, with an average size (± standard deviation) of 18332 (± 56870) acres. Numerical IDs for each HEVA are given in Figure 2 and correspond to IDs in Table 1, which provides average values of all indicators, as well as the composite index, for each HEVA. Indicator means and standard deviations in Table 1 are presented as standardized values (i.e., z-scores, see Section 3 above) to facilitate direct comparison of values between indicators and across HEVAs. Indicator values in their original units (e.g., metric tons of carbon per hectare for total carbon) are presented in **Appendix B**. **Appendix C** contains several additional maps, including the unsmoothed composite index layer (Fig. C1), satellite imagery (Fig. C2), and roads and trails (Fig. C3), providing further context for our model results. Spatial data developed for this project, including the smoothed composite index and HEVAs, are available here:

It is important to note that our determinations of areas of high ecological value within the Shasta-Trinity National Forest are relative in the sense that, if an area within the forest is not identified as a HEVA (i.e., does not have composite index values within the top 10%) this does not imply that the area has low importance for ecology and conservation. Rather, it means that the combination of all indicator values considered here is relatively low in that area as compared to other areas within the forest. It is also worth reiterating that, as with all model-based indices, the results of our composite index of ecological value will depend on the exact indicators used and the relative importance values they are assigned. We have endeavored to (1) use a comprehensive set of literature-supported indicators that reflect a broad range of ecological values, and (2) ensure that all indicators have equal influence in determining the value of the resulting index. However, we note that the use of other or additional indicators, or the selection of weights that emphasize the importance of certain indicators over others, would likely lead to somewhat different results. Finally, we note that, while we have confidence in the underlying datasets used to identify HEVAs, these areas have not been subjected to ground-truthing to verify their ecological value.

Given these considerations, we expect that the delineation of HEVAs in this report will be useful in identifying potential areas for conservation-focused management within the Shasta-Trinity National Forest. HEVAs can serve as a starting point for understanding which unprotected areas on the forest are likely to be the most important for ensuring its long-term ecological sustainability. By considering HEVAs, the Forest Service, in collaboration with stakeholders, can design management plans that ensure the continued presence of the ecological values represented by our indicator variables during the agency's forest plan revision process. Because HEVAs consider only ecological aspects, it is important that the Forest Service and stakeholders include additional social and economic sustainability considerations when determining the appropriateness of a given HEVA for increased conservation or any other management emphasis. These social and economic considerations are best applied during the forest plan revision process through stakeholder input received by the Forest Service. This research provides a useful starting point for those discussions.
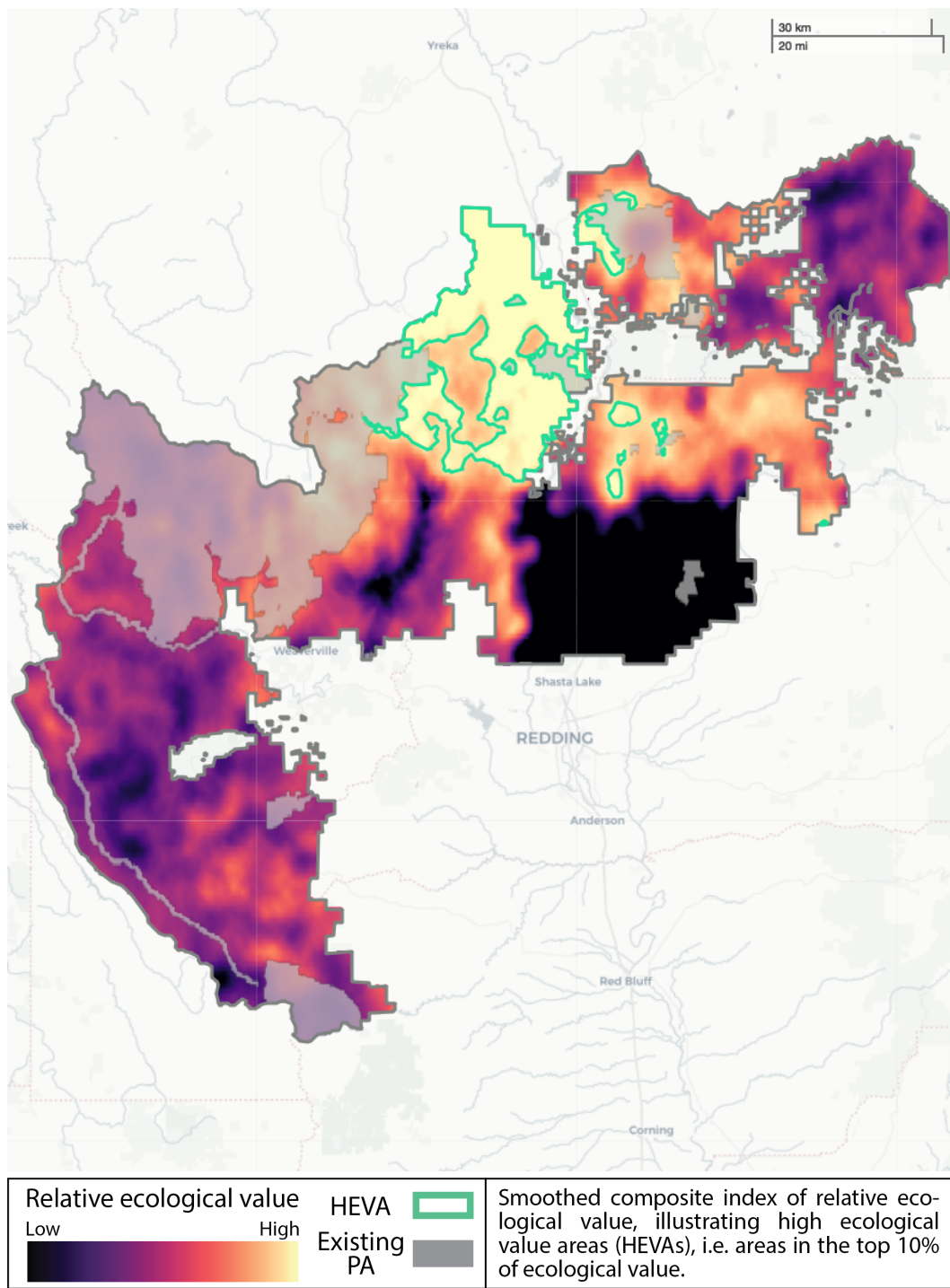
Figure 1. Map of Shasta-Trinity National Forest showing the smoothed composite index of ecological value. See the reference map (Fig. 2) for HEVA labels, corresponding to rows in Table 1.
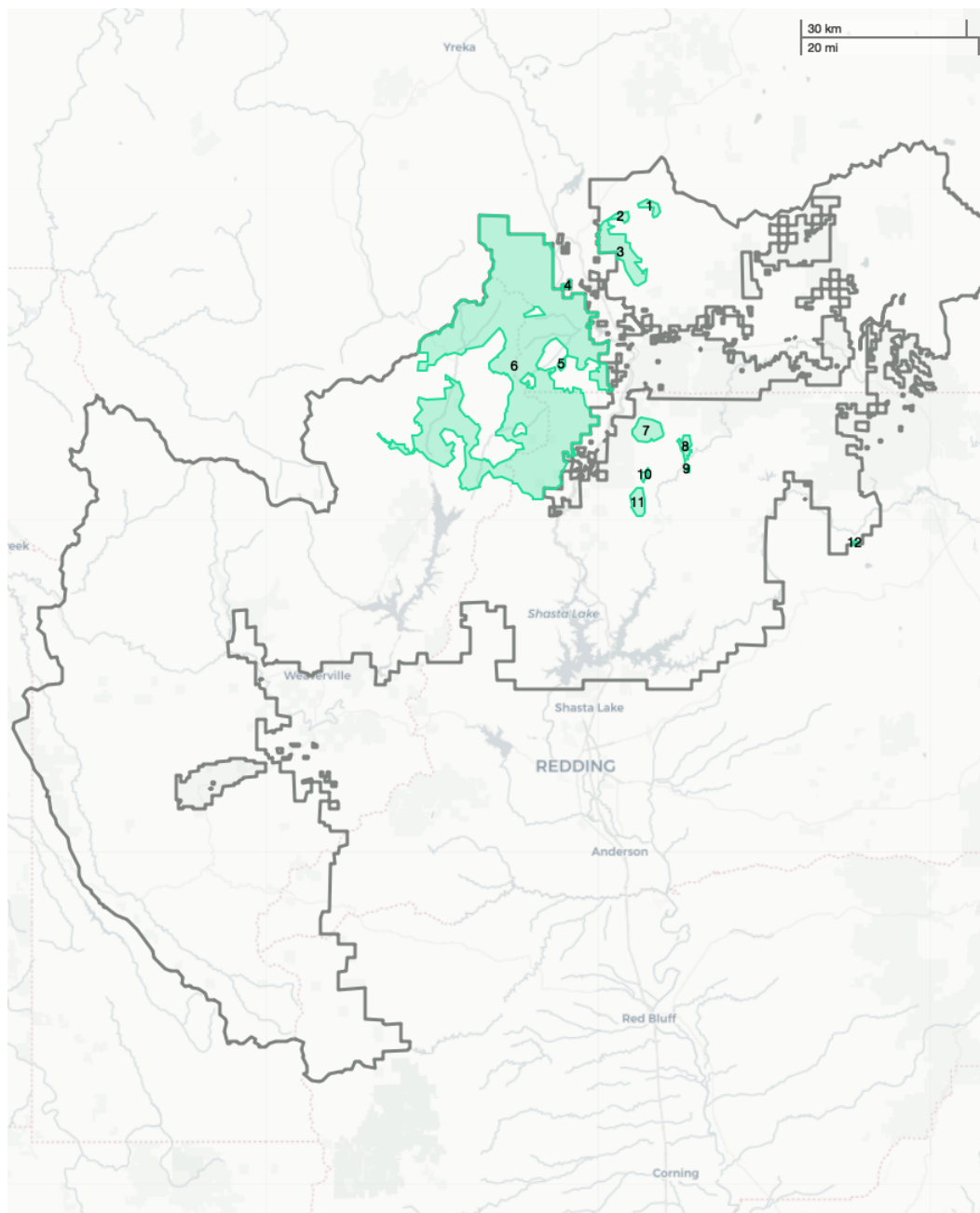
Figure 2. Reference map showing the ID for each HEVA in Fig. 1, with ID numbers increasing from north to south. IDs correspond to those in Table 1.

Table 1. Summary statistics for all high ecological value areas (HEVAs). HEVA IDs correspond to the numeric labels in the reference map (Fig. 2). Values for ecological and environmental indicators and the composite index are given as means (standard deviations) for all pixels within the HEVA. Indicator means are shown as standardized (i.e., z-transformed) values, as described in Section 3 above. Standardized indicator values are comparable across indicators and HEVAs. HEVA area is given in acres. See Section 4 above for a description of road impacts.

ID	Area	% NFS lands	Road impact	Climate resilience	Connectivity	Imperiled richness	Intactness	Total carbon	Vegetation diversity	Vertebrate richness	Composite Index
1	1321	84	0.05	0.6 (0.02)	0.56 (0.81)	-0.17 (0.19)	0.01 (0.75)	0.06 (0.51)	1.14 (0.09)	0.55 (0.1)	0.39 (0.13)
2	903	93	0.04	0.56 (0.03)	0.7 (0.39)	0.02 (0.21)	0.4 (0.3)	0.09 (0.51)	1.14 (0.06)	0.76 (0)	0.5 (0.13)
3	9221	81	0.05	0.59 (0.05)	0.04 (0.63)	-0.1 (0.33)	0.12 (0.65)	0.2 (0.52)	0.95 (0.14)	0.75 (0.02)	0.43 (0.14)
4	306	99	0.03	0.47 (0.02)	-0.29 (0.6)	-0.28 (0)	-0.55 (0.67)	0.96 (0.37)	1.01 (0.06)	0.8 (0.04)	0.48 (0.15)
5	444	100	0.00	0.61 (0.01)	0.46 (0.21)	-0.38 (0.2)	0.57 (0.09)	0.92 (0.48)	0.45 (0.12)	0.39 (0.08)	0.43 (0.09)
6	198731	70	0.04	0.58 (0.06)	0.42 (0.47)	-0.01 (0.56)	0.23 (0.6)	0.73 (0.72)	0.73 (0.36)	0.44 (0.15)	0.48 (0.17)
7	4258	93	0.01	0.55 (0.06)	0.65 (0.26)	-0.73 (0)	0.44 (0.43)	1.61 (0.62)	0.1 (0.13)	0.23 (0.02)	0.39 (0.14)
8	1531	100	0.00	0.48 (0.01)	0.53 (0.08)	-0.73 (0)	0.75 (0.01)	1.55 (0.78)	0.09 (0.05)	0.17 (0.02)	0.4 (0.16)
9	146	98	0.00	0.52 (0.01)	0.5 (0.07)	-0.73 (0)	0.74 (0.01)	1.75 (0.61)	0.22 (0.04)	0.1 (0)	0.46 (0.13)
10	376	100	0.00	0.61 (0.02)	0.85 (0.22)	-0.73 (0)	0.76 (0)	1.38 (0.66)	0.29 (0.06)	0.22 (0.01)	0.43 (0.14)
11	2549	99	0.00	0.63 (0)	0.97 (0.18)	-0.73 (0)	0.76 (0)	1.42 (0.7)	0.27 (0.07)	0.18 (0.04)	0.43 (0.15)
12	202	61	0.00	0.54 (0.01)	0.27 (0.28)	-0.73 (0)	0.75 (0)	1.53 (0.85)	0.11 (0.04)	-0.23 (0.05)	0.35 (0.18)

Acknowledgments

Literature cited

AdaptWest Project. 2015. Gridded climatic velocity data for North America at 1km resolution. Available at adaptwest.databasin.org.

Anderson-Teixeira, K. J., M. M. H. Wang, J. C. McGarvey, V. Herrmann, A. J. Tepley, B. Bond-Lamberty, and D. S. LeBauer. 2018. ForC: a global database of forest carbon stocks and fluxes. Ecology 99:1507–1507.

Angermeier, P. L., and J. R. Karr. 1996. Biological integrity versus biological diversity as policy directives: Protecting biotic resources. Pages 264–275 in F. B. Samson and F. L. Knopf, editors. Ecosystem Management: Selected Readings. Springer, New York, NY.

Becker, W., M. Saisana, P. Paruolo, and I. Vandecasteele. 2017. Weights and importance in composite indicators: Closing the gap. Ecological Indicators 80:12–22.

Burgass, M. J., B. S. Halpern, E. Nicholson, and E. J. Milner-Gulland. 2017. Navigating uncertainty in environmental composite indicators. Ecological Indicators 75:268–278.

Carroll, C., J. J. Lawler, D. R. Roberts, and A. Hamann. 2015. Biotic and climatic velocity identify contrasting areas of vulnerability to climate change. PLOS ONE 10:e0140486.

Comer, P. 2003. Ecological systems of the United States: A working classification of U.S. terrestrial systems. NatureServe, Arlington, VA.

CSP. 2019. Methods and approach used to estimate the loss and fragmentation of natural lands in the conterminous U.S. from 2001 to 2017. Technical Report, Truckee, CA.

Dickson, B. G., C. M. Albano, R. Anantharaman, P. Beier, J. Fargione, T. A. Graves, M. E. Gray, K. R. Hall, J. J. Lawler, P. B. Leonard, C. E. Littlefield, M. L. McClure, J. Novembre, C. A. Schloss, N. H. Schumaker, V. B. Shah, and D. M. Theobald. 2019. Circuit-theory applications to connectivity science and conservation. Conservation Biology 33:239–249.

Dickson, B. G., C. M. Albano, B. H. McRae, J. J. Anderson, D. M. Theobald, L. J. Zachmann, T. D. Sisk, and M. P. Dombeck. 2017. Informing strategic efforts to expand and connect protected areas using a model of ecological flow, with application to the western United States. Conservation Letters 10:564–571.

Dickson, B. G., L. J. Zachmann, and C. M. Albano. 2014. Systematic identification of potential conservation priority areas on roadless Bureau of Land Management lands in the western United States. Biological Conservation 178:117–127.

Forman, R. T. T. 2000. Estimate of the Area Affected Ecologically by the Road System in the United States. Conservation Biology 14:31–35.

Forman, R. T. T., and L. E. Alexander. 1998. Roads and their major ecological effects. Annual Review of Ecology and Systematics 29:207–231.

Goldstein, A., W. R. Turner, S. A. Spawn, K. J. Anderson-Teixeira, S. Cook-Patton, J. Fargione, H. K. Gibbs, B. Griscom, J. H. Hewson, J. F. Howard, J. C. Ledezma, S. Page, L. P. Koh, J. Rockström, J. Sanderman, and D. G. Hole. 2020. Protecting irrecoverable carbon in Earth's ecosystems. Nature Climate Change 10:287–295.

Greco, S., A. Ishizaka, M. Tasiou, and G. Torrisi. 2019. On the methodological framework of composite indices: A review of the issues of weighting, aggregation, and robustness. Social Indicators Research 141:61–94.

Hamann, A., D. R. Roberts, Q. E. Barber, C. Carroll, and S. E. Nielsen. 2015. Velocity of climate change algorithms for guiding conservation and management. Global Change Biology 21:997–1004.

Heller, N. E., and E. S. Zavaleta. 2009. Biodiversity management in the face of climate change: A review of 22 years of recommendations. Biological Conservation 142:14–32.

Hengl, T., J. M. de Jesus, G. B. M. Heuvelink, M. R. Gonzalez, M. Kilibarda, A. Blagotić, W. Shangguan, M. N. Wright, X. Geng, B. Bauer-Marschallinger, M. A. Guevara, R. Vargas, R. A. MacMillan, N. H. Batjes, J. G. B. Leenaars, E. Ribeiro, I. Wheeler, S. Mantel, and B. Kempen. 2017. SoilGrids250m: Global gridded soil information based on machine learning. PLOS ONE 12:e0169748.

Jung, M., P. R. Dahal, S. H. M. Butchart, P. F. Donald, X. De Lamo, M. Lesiv, V. Kapos, C. Rondinini, and P. Visconti. 2020. A global map of terrestrial habitat types. Scientific Data 7:256.

KBA Standards and Appeals Committee. 2019. Guidelines for using a Global Standard for the Identification of Key Biodiversity Areas. Page 148. Prepared by the KBA Standards and Appeals Committee of the IUCN Species Survival Commission and IUCN World Commission on Protected Areas, Gland, Switzerland.

Landau, V. A., V. B. Shah, R. Anantharaman, and K. R. Hall. 2021. Omniscape.jl: Software to compute omnidirectional landscape connectivity. Journal of Open Source Software 6:2829.

McRae, B. H., B. G. Dickson, T. H. Keitt, and V. B. Shah. 2008. Using circuit theory to model connectivity in ecology, evolution, and conservation. Ecology 89:2712–2724.

McRae, B., K. Popper, A. Jones, M. Schindel, S. Buttrick, K. Hall, R. Unnasch, and J. Platt. 2016. Conserving nature's stage: Mapping omnidirectional connectivity for resilient terrestrial landscapes in the Pacific Northwest. The Nature Conservancy, Portland, OR.

Mokany, K., R. J. Raison, and A. S. Prokushkin. 2006. Critical analysis of root : shoot ratios in terrestrial biomes. Global Change Biology 12:84–96.

Mykleby, P. M., P. K. Snyder, and T. E. Twine. 2017. Quantifying the trade-off between carbon sequestration and albedo in midlatitude and high-latitude North American forests. Geophysical Research Letters 44:2493–2501.

NatureServe. 2020. Map of Biodiversity Importance. Arlington, VA.

Noon, M., A. Goldstein, J. Ledezma, P. Roehrdanz, S. Cook-Patton, S. Spawn-Lee, T. Wright, M. Gonzalez-Roglich, D. Hole, J. Rockström, and W. Turner. 2021. Mapping the irrecoverable carbon in Earth's ecosystems. under review.

Noss, R. F. 1990. Indicators for Monitoring Biodiversity: A Hierarchical Approach. Conservation Biology 4:355–364.

Parrish, J. D., D. P. Braun, and R. S. Unnasch. 2003. Are we conserving what we say we are? Measuring ecological integrity within protected areas. BioScience 53:851–860.

Paruolo, P., M. Saisana, and A. Saltelli. 2013. Ratings and rankings: voodoo or science? Journal of the Royal Statistical Society: Series A (Statistics in Society) 176:609–634.

Shanley, C. S., and S. Pyare. 2011. Evaluating the road-effect zone on wildlife distribution in a rural landscape. Ecosphere 2:art16.

Soto-Navarro, C., C. Ravilious, A. Arnell, X. de Lamo, M. Harfoot, S. L. L. Hill, O. R. Wearn, M. Santoro, A. Bouvet, S. Mermoz, T. Le Toan, J. Xia, S. Liu, W. Yuan, S. A. Spawn, H. K. Gibbs, S. Ferrier, T. Harwood, R. Alkemade, A. M. Schipper, G. Schmidt-Traub, B. Strassburg, L. Miles, N. D. Burgess, and V. Kapos. 2020. Mapping co-benefits for carbon storage and biodiversity to inform conservation policy and action. Philosophical Transactions of the Royal Society B: Biological Sciences 375:20190128.

Spawn, S. A., C. C. Sullivan, T. J. Lark, and H. K. Gibbs. 2020. Harmonized global maps of above and belowground biomass carbon density in the year 2010. Scientific Data 7:112.

Theobald, D. M. 2010. Estimating natural landscape changes from 1992 to 2030 in the conterminous US. Landscape Ecology 25:999–1011.

Theobald, D. M. 2013. A general model to quantify ecological integrity for landscape assessments and US application. Landscape Ecology 28:1859–1874.

Theobald, D. M., D. Harrison-Atlas, W. B. Monahan, and C. M. Albano. 2015. Ecologically-relevant maps of landforms and physiographic diversity for climate adaptation planning. PLOS ONE 10:e0143619.

U.S. Census Bureau 2019, TIGER/Line Shapefiles. https://www.census.gov/geographies/mapping-files/time-series/geo/tiger-line-file.html

USGS. 2011. National Gap Analysis Program Land Cover Data- Version 2. Available from http://gapanalysis.usgs.gov/gaplandcover/.

Wilderness Act, 1964; 78 Stat. 890; United States Statutes at Large, Volume 78, 88th Congress, 2nd Session; An Act to establish a National Wilderness Preservation System for the permanent good of the whole people, and for other purposes; Public Law 88-577.

Williams, C. A., H. Gu, and T. Jiao. 2021. Climate impacts of U.S. forest loss span net warming to net cooling. Science Advances 7:eaax8859.

Xia, J., S. Liu, S. Liang, Y. Chen, W. Xu, and W. Yuan. 2014. Spatio-temporal patterns and climate variables controlling of biomass carbon stock of global grassland ecosystems from 1982 to 2006. Remote Sensing 6:1783–1802.

Appendix A: Optimizing indicator weights for equal importance in composite indices

We used a composite index approach (see Greco et al. 2019) to combine several individual indicators into a single metric of ecological value. In our case, we used a simple linear combination of indicators with weights applied to each indicator. The values of the composite index, *y* (a column vector of length *I*), are calculated as

$$y = Xw \qquad\qquad \text{(eq. A1)}$$

X is an *I* × *J* matrix of indicator values, where x_{ij} is the value of indicator *j* for observation *i*, and *w* is a column vector of weights of length *J*, where w_j is the weight for indicator *j*. The observations, *i*, in our case correspond to the values of individual pixels in spatially-gridded indicator data.

It is tempting to assume, in the case of the linear combination in equation A1, that the weights represent the relative importance of each indicator in determining the overall composite index, but this is not always the case (Paruolo et al. 2013, Becker et al. 2017). When indicators are correlated, weights are often not truly representative of importance. Paruolo et al. (2013) and Becker et al. (2017) offer a simple metric of "importance", S_j, for indicator *j*, that accommodates correlation among indicators:

$$S_j = \frac{\sum_{i=1}^{I}\left(E\left(\hat{y}_i\middle|x_{ij}\right)-\bar{y}\right)^2}{\sum_{i=1}^{I}\left(y_i-\bar{y}\right)^2} \qquad\qquad \text{(eq. A2)}$$

S_j, also called the Pearson correlation ratio, is a measure of the degree to which a single indicator can explain observed variation in the composite index, *y*. $E(\hat{y}_i \mid x_{ij})$ is the expected value of the composite index given the value of indicator *j* for observation *i*, $\bar{y}$ is the mean observed composite index value across all observations, and y_i is the observed composite index value for the *i*[th] observation. $E(\hat{y}_i \mid x_{ij})$ can be defined using any regression of indicator *j* on *y*, including nonlinear and non-parametric regression. This feature is important because – in the case of correlated indicators – the relationship between indicator *j* and the composite index *y* can be nonlinear. Becker et al. (2017) suggest that Gaussian process or penalised splines regression offer the most generalizable solution for defining $E(\hat{y}_i \mid x_{ij})$ because it can accommodate highly complex nonlinear correlations among indicators. For our purposes, we found that polynomial regression with degree 4 could sufficiently capture nonlinear relationships between indicators and composite index scores resulting from correlations among

indicators. We opted to use this simpler regression function because it is less subject to parameterization decisions than penalized splines (e.g. number of knots, degree, and order) and offers vast improvements in computation speed compared to Gaussian process regression.

With Eq. A2, we now have a way to measure the *importance* of each indicator. Following Becker et al. (2017), we use an optimization algorithm to determine the set of weights that yields, based on equation A2, the desired set of importances (i.e., those chosen by the user, in this case, equal importance across all indicators). Specifically, we used the Nelder Mead function (with bounds [0, 1] for individual weights) in the lme4 package in R (Bates et al. 2015), and optimized weights to determine the set of weights that minimizes the difference between our desired importances (i.e., equal importance) and observed importances (the values of S_j). There is not always a perfect solution to the "inverse problem" (Paruolo et al. 2013), but the optimizer will nonetheless find the "best" solution. For this reason, it is important to verify using equation A2 that the optimal weights do indeed result in importances that are acceptably close to the desired importances.

As noted in the main text above, for the analysis described here, we used equal importance as the basis for all indicators in our composite index, as there was no *a priori* justification for applying different importance values to different indicators. In other applications, the process of determining weights is often expert-driven. It may be necessary in such cases to solicit expert opinion on what the desired *importances* should be, rather than weights, as it is much more intuitive.

References for Appendix A

Bates, D., D. Sarkar, M. D. Bates, and L. Matrix. 2007. The lme4 package. R package version, 2:74.

Becker, W., M. Saisana, P. Paruolo, and I. Vandecasteele. 2017. Weights and importance in composite indicators: Closing the gap. Ecological indicators, 80:12–22.

Greco, S., A. Ishizaka, M. Tasiou, and G. Torrisi. 2019. On the methodological framework of composite indices: A review of the issues of weighting, aggregation, and robustness. Social Indicators Research, 141:61–94.

Paruolo, P., M. Saisana, and A. Saltelli. 2013. Ratings and rankings: voodoo or science? Journal of the Royal Statistical Society: Series A (Statistics in Society), 176:609–634.

Appendix B: HEVA summary statistics with original scale indicators

Table B1. Summary statistics for all high ecological value areas (HEVAs). HEVA IDs correspond to the numeric labels in the reference map (Fig. 2). Values for ecological and environmental indicators and the composite index are given as means (standard deviations) for all pixels within the HEVA. Indicator means are shown in their original units (i.e., not z-transformed), as described in Section 3 above. HEVA area is given in acres. See Section 4 above for a description of road impacts.

ID	Area	% NFS lands	Road impact	Climate resilience	Connectivity	Imperiled richness	Intactness	Total carbon	Vegetation diversity	Vertebrate richness	Composite Index
1	1321	84	0.05	-0.23 (0.07)	6272.97 (1575.43)	1.24 (0.43)	0.86 (0.14)	119.42 (27.01)	0.34 (0.01)	96.6 (1.7)	0.39 (0.13)
2	903	93	0.04	-0.38 (0.13)	6529.41 (745.74)	1.66 (0.47)	0.93 (0.05)	121.02 (27.32)	0.34 (0)	100 (0)	0.5 (0.13)
3	9221	81	0.05	-0.27 (0.25)	5262.68 (1213.75)	1.39 (0.73)	0.88 (0.12)	127.2 (27.57)	0.33 (0.01)	99.89 (0.31)	0.43 (0.14)
4	306	99	0.03	-0.79 (0.09)	4610.1 (1157.84)	1 (0)	0.76 (0.12)	167.48 (19.97)	0.33 (0)	100.72 (0.64)	0.48 (0.15)
5	444	100	0.00	-0.15 (0.04)	6070.21 (405.22)	0.77 (0.45)	0.96 (0.02)	165.41 (25.54)	0.29 (0.01)	93.81 (1.32)	0.43 (0.09)
6	198731	70	0.04	-0.3 (0.28)	5999.49 (919.15)	1.6 (1.24)	0.9 (0.11)	154.93 (38.65)	0.31 (0.02)	94.64 (2.48)	0.48 (0.17)
7	4258	93	0.01	-0.43 (0.25)	6435.43 (505.16)	0 (0)	0.93 (0.08)	202.09 (33.01)	0.27 (0.01)	91.19 (0.4)	0.39 (0.14)
8	1531	100	0.00	-0.77 (0.05)	6211.45 (157.95)	0 (0)	0.99 (0)	198.92 (41.61)	0.27 (0)	90.17 (0.38)	0.4 (0.16)
9	146	98	0.00	-0.59 (0.03)	6157.67 (133.55)	0 (0)	0.99 (0)	209.79 (32.49)	0.28 (0)	89 (0)	0.46 (0.13)
10	376	100	0.00	-0.15 (0.1)	6817.54 (429.77)	0 (0)	0.99 (0)	190.11 (35.38)	0.28 (0)	90.95 (0.22)	0.43 (0.14)
11	2549	99	0.00	-0.08 (0.02)	7053.37 (356.18)	0 (0)	0.99 (0)	191.9 (37.06)	0.28 (0)	90.4 (0.72)	0.43 (0.15)
12	202	61	0.00	-0.5 (0.02)	5705.51 (535.07)	0 (0)	0.99 (0)	197.97 (45.21)	0.27 (0)	83.5 (0.84)	0.35 (0.18)

Appendix C. Additional maps

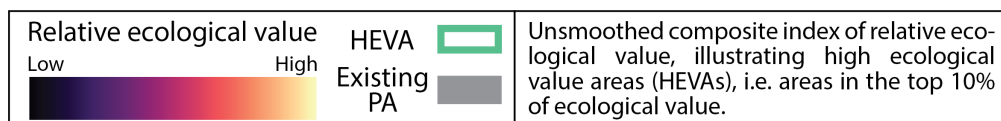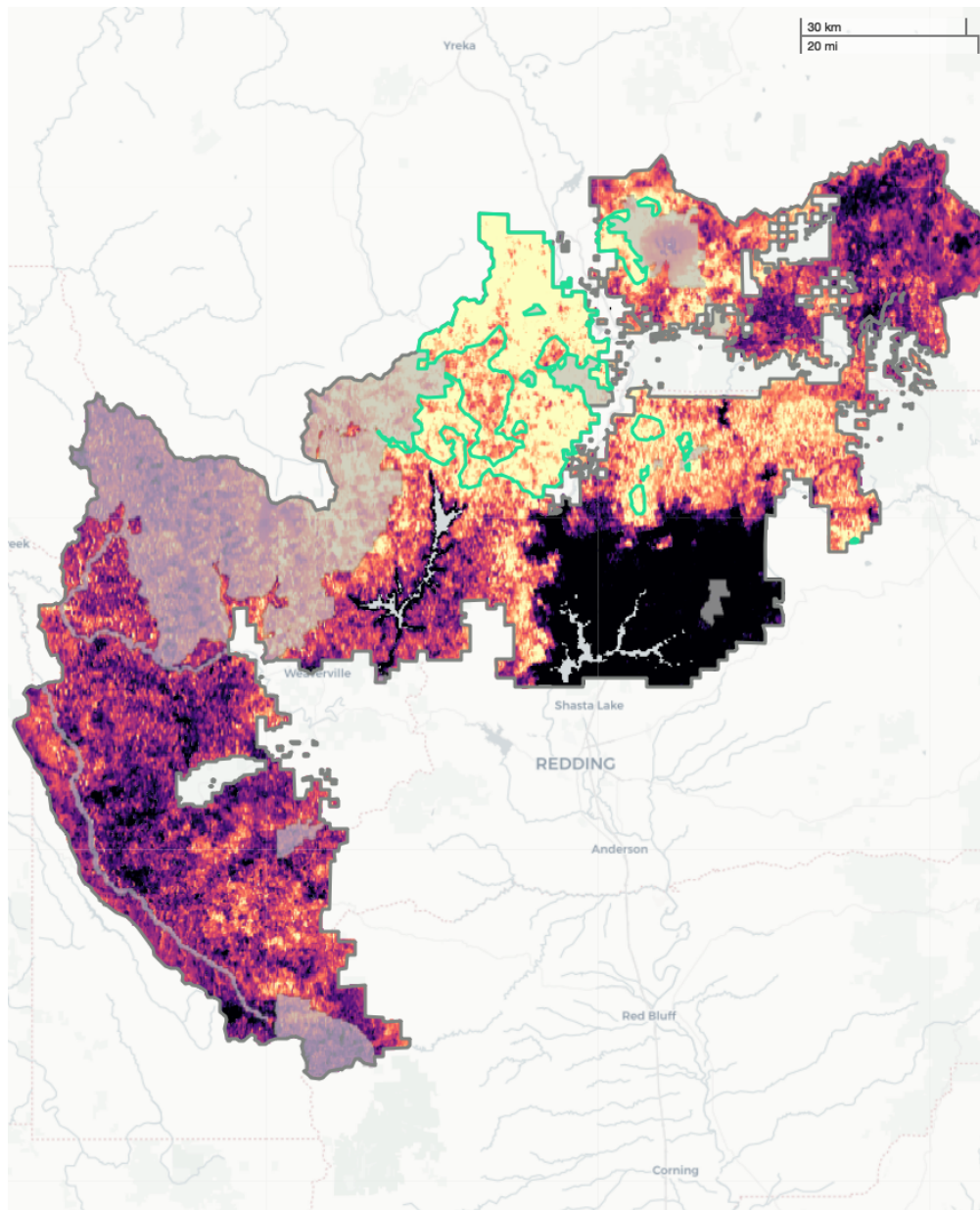| Relative ecological value | HEVA | Unsmoothed composite index of relative eco- |
| Low   High | Existing PA | logical value, illustrating high ecological value areas (HEVAs), i.e. areas in the top 10% of ecological value. |

Figure C1. Map of Shasta-Trinity National Forest showing the unsmoothed composite index of ecological value, with HEVAs (i.e., areas in the top 10% of ecological value) outlined in green. Existing protected areas (PAs) are shown as shaded gray regions. See the reference map (Fig. 2) for HEVA IDs, corresponding to rows in Table 1.
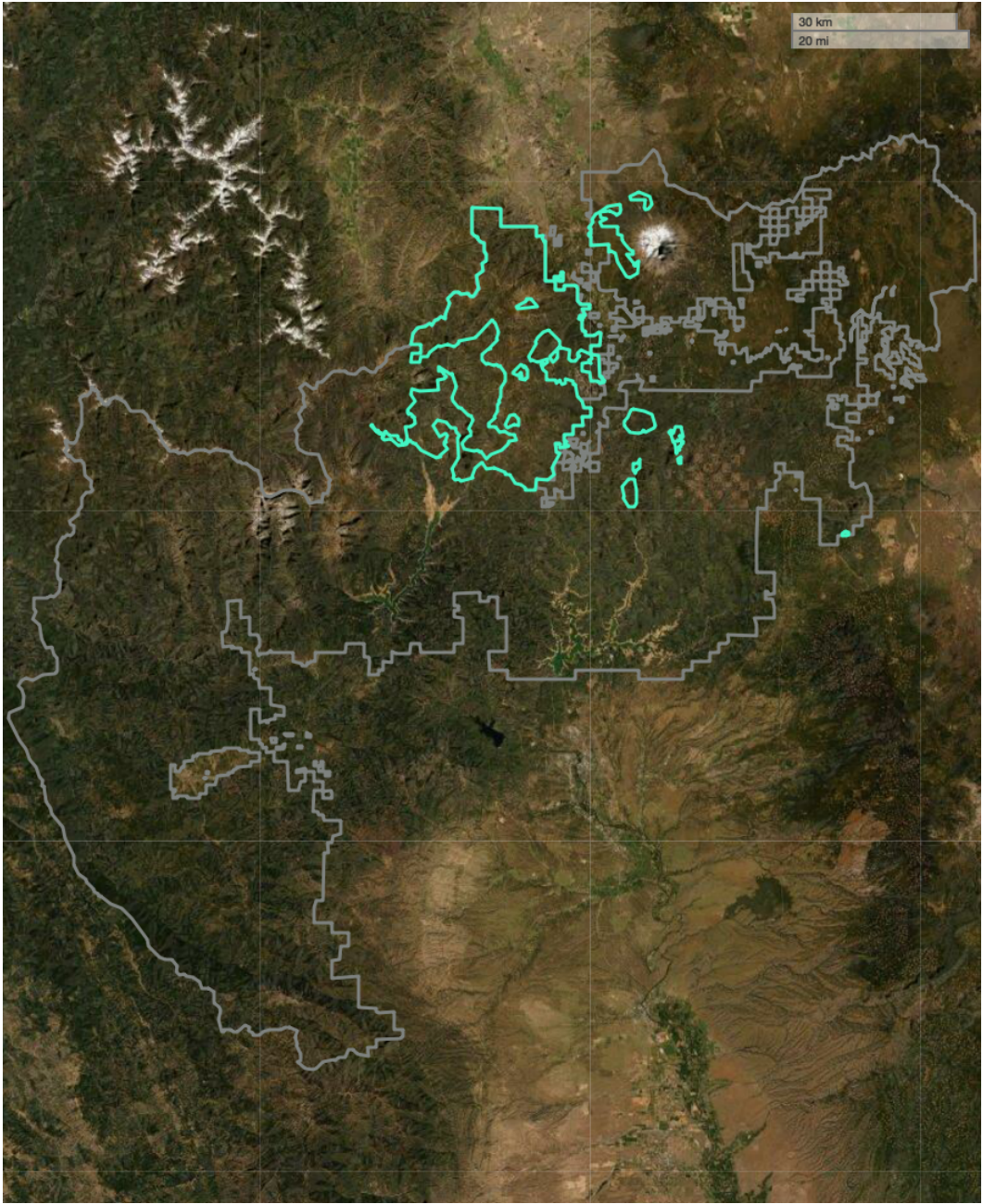
Figure C2. Satellite map of Shasta-Trinity National Forest showing HEVAs (i.e., areas in the top 10% of ecological value) as green polygons. See the reference map (Fig. 2) for HEVA IDs, corresponding to rows in Table 1.
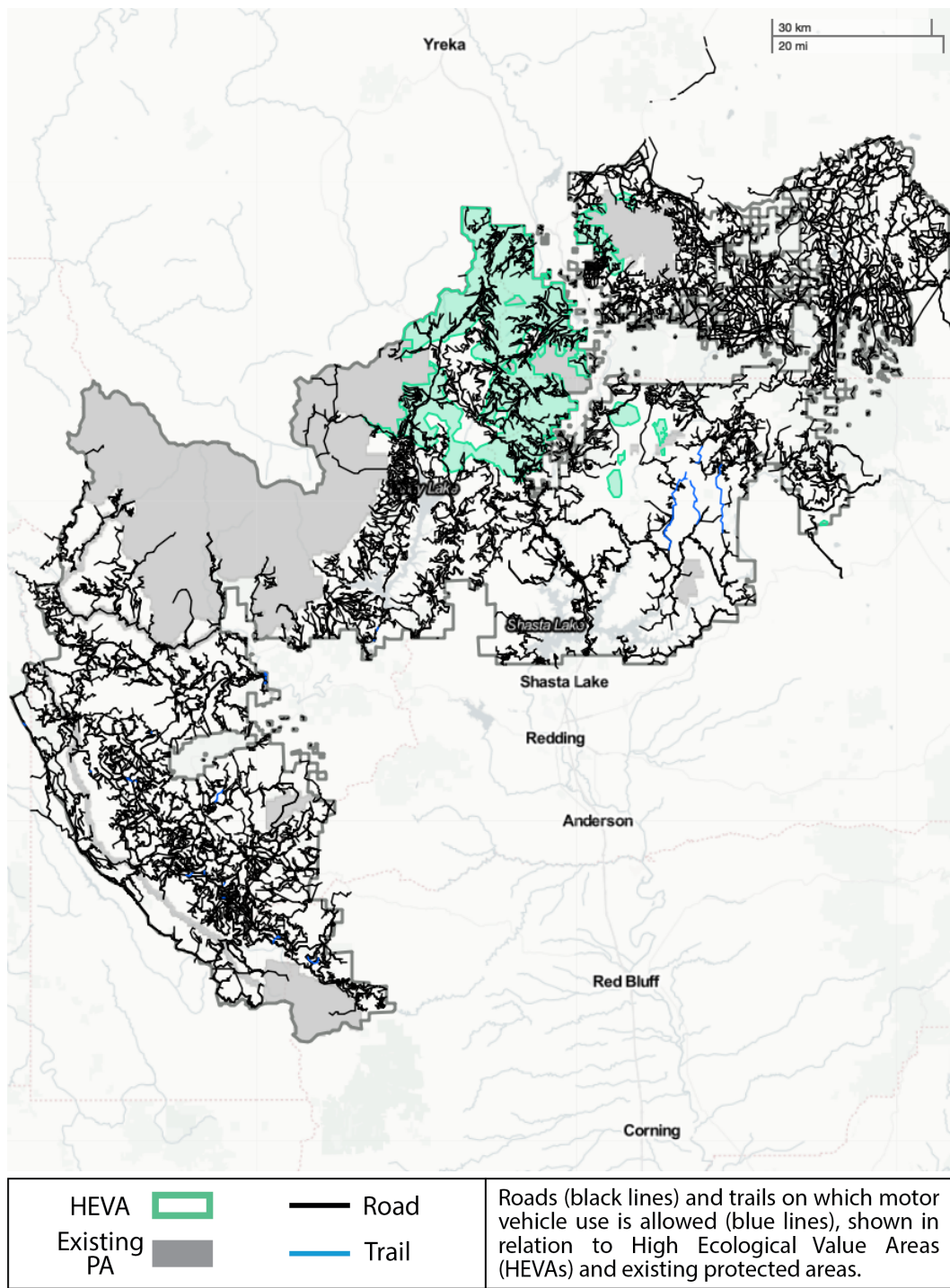
Figure C3. Map of Shasta-Trinity National Forest showing roads and trails. See the reference map (Fig. 2) for HEVA IDs, corresponding to rows in Table 1.